Published in final edited form as:
Cancer Res. 2013 May 15; 73(10): 3155–3167. doi:10.1158/0008-5472.CAN-12-3266.

Trop-2 promotes prostate cancer metastasis by modulating β_1 integrin functions

Marco Trerotola[1,2], **Danielle L. Jernigan**[3], **Qin Liu**[4], **Javed Siddiqui**[5,6], **Alessandro Fatatis**[2,3,7], and **Lucia R. Languino**[1,2,*]

[1]Prostate Cancer Discovery and Development Program, Department of Cancer Biology, Philadelphia, Pennsylvania

[2]Kimmel Cancer Center, Thomas Jefferson University; Philadelphia, Pennsylvania

[3]Department of Pharmacology and Physiology, Drexel University College of Medicine; Philadelphia, Pennsylvania

[4]Prostate Cancer Discovery and Development Program, and Molecular and Cellular Oncogenesis Program, The Wistar Institute Cancer Center, Philadelphia, Pennsylvania

[5]Michigan Center for Translational Pathology, Ann Arbor, Michigan

[6]Department of Pathology, University of Michigan Medical School, Ann Arbor, Michigan

[7]Department of Pathology and Laboratory Medicine, Drexel University College of Medicine, Philadelphia, Pennsylvania

Abstract

The molecular mechanisms underlying metastatic dissemination are still not completely understood. We have recently shown that β_1 integrin-dependent cell adhesion to fibronectin (FN) and signaling are affected by a transmembrane molecule, Trop-2, which is frequently upregulated in human carcinomas. Here we report that Trop-2 promotes metastatic dissemination of prostate cancer cells in vivo and is abundantly expressed in metastasis from human prostate cancer. We also show here that Trop-2 promotes prostate cancer cell migration on FN, a phenomenon dependent on β_1 integrins. Mechanistically, we demonstrate that Trop-2 and the $\alpha_5\beta_1$ integrin associate through their extracellular domains, causing relocalization of $\alpha_5\beta_1$ and the β_1-associated molecule talin from focal adhesions to the leading edges. Trop-2 effect is specific since this molecule does not modulate migration on vitronectin (VN), does not associate with the major VN receptor, $\alpha_v\beta_3$ integrin, and does not affect localization of $\alpha_v\beta_3$ integrin as well as vinculin in focal adhesions. We show that Trop-2 enhances directional prostate cancer cell migration, through modulation of Rac1 GTPase activity. Finally, we demonstrate that Trop-2 induces activation of

*Corresponding Author: Lucia R. Languino Ph.D., Department of Cancer Biology, Thomas Jefferson University, 233 South 10th Street, Philadelphia, PA 19107. Phone: 215.503.3442. Fax: 215.503.1607. lucia.languino@jefferson.edu.

Conflicts of Interest: No potential conflicts of interest are disclosed.

Authors' Contributions

Conception and design: M. Trerotola and LR. Languino.
Development of methodology: M. Trerotola performed all experiments with the exception of intracardiac cell injections, performed by D. Jernigan.
Acquisition of data: M. Trerotola.
Analysis and interpretation of data: M. Trerotola, A. Fatatis and LR. Languino.
Writing, review, and/or revision of the manuscript: M. Trerotola and LR. Languino.
Administrative, technical, or material support: J. Siddiqui for having provided tissue microarrays.
Study supervision: LR. Languino.
Other: Q. Liu for statistical analysis.

PAK4, a kinase that has been reported to mediate cancer cell migration. In conclusion, we provide the first evidence that β_1 integrin-dependent migratory and metastatic competence of prostate cancer cells is enhanced by Trop-2.

Introduction

Prostate cancer is a significant cause of cancer morbidity and mortality in men in the United States. In 2013, more than 238,000 men are expected to be diagnosed with prostate cancer and more than 29,000 men are estimated to die from this disease (1), mostly due to metastatic dissemination in distant organs. The molecular mechanisms underlying metastatic spreading are still not completely understood. However, loss of intercellular contacts and acquisition of enhanced capacity to migrate on extracellular matrix (ECM) substrates represent critical steps for the onset of the metastatic cascade (2–4). The integrin family of transmembrane receptors mediates interaction between cells and ECM. Integrins are heterodimers generated by the noncovalent association between one of the 18 α and one of the 8 β subunits (5). Each integrin heterodimer has the ability to recognize and bind multiple ligands, and mediate cell adhesion, spreading and migration through modulation of several intracellular signaling pathways (5). Efficient cell migration on ECM substrates requires dynamic turnover of focal adhesions, assembled at cell-ECM contacts. These structures are macromolecular complexes of integrins and other transmembrane receptors linked to the actin cytoskeleton through several adaptors (6). Since integrins are central regulators of focal adhesion dynamics, changes of their expression profiles and/or activities in cancer represent a functionally relevant contribution to the metastatic dissemination (7–9).

The major fibronectin (FN) receptor, $\alpha_5\beta_1$ integrin, plays a critical role during cancer progression, promoting migratory and invasive phenotypes, and generation of contractile forces (10). In prostate cancer, inactivation of $\alpha_5\beta_1$ integrin with blocking antibodies (Abs) has been reported to be responsible for reduced motility of aggressive C4-2 cells on FN (11). This suggests that the FN – $\alpha_5\beta_1$ axis may be a target for therapeutic approaches against aggressive cancer.

Trop-2 is a type-I transmembrane glycoprotein that comprises an extracellular domain covering most protein sequence, a single hydrophobic transmembrane helix and a 26-aa intracytoplasmic C-terminal tail. Within the extracellular portion of Trop-2 there are two distinct motifs, designated as GA733 type-1 and thyroglobulin type-1A, and also detected in the Trop-2 paralog, Trop-1/EpCAM (12). The intracytoplasmic domain of Trop-2 contains a HIKE motif for binding to pleckstrin homology domains and a PKC phosphorylation site (13). The Trop molecules modulate cell-cell adhesion through homophilic interactions between multimers localized on the surface of adjacent cells, and interact with tight junction proteins (14). mRNA and protein levels of Trop-2, recently analyzed in several human carcinomas, are upregulated in most cancer tissues as compared with their normal counterparts (15). This upregulation results in accelerated tumor growth and correlates with poor prognosis (15). We and other investigators have shown that Trop-2 is predominantly expressed in the basal layer of the benign human prostatic epithelium (16, 17). However, Trop-2 is significantly upregulated in prostate cancer as compared with benign luminal cells (15, 16), which give rise to prostate cancer. This evidence suggests a role for Trop-2 during disease progression.

We have recently demonstrated that Trop-2 modulates β_1 integrin-mediated attachment of prostate cancer cells to FN; specifically, Trop-2 appears to function as an anti-adhesive molecule on this ECM ligand (18). This evidence and the observation that mutations of the *TROP2* gene are responsible for a hereditary corneal amyloidosis known as Gelatinuos

Drop-Like Dystrophy, characterized by altered ECM and integrin distribution (19), suggest that Trop-2 modulates not only cell-cell but also cell-ECM interactions. Here we show that Trop-2 promotes metastatic dissemination of prostate cancer cells in vivo; consistently, we observe that this molecule is abundantly expressed in human prostate cancer metastases to various organs. Trop-2 is shown here to stimulate directional migration of prostate cancer cells on FN through relocalization of $\alpha_5\beta_1$ integrin and its associated molecule talin from focal adhesions to the leading edges. In conclusion, our findings demonstrate an active role for Trop-2 in promoting metastatic dissemination of prostate cancer cells, and candidate this molecule as a novel biomarker of aggressive disease.

Materials and Methods

Reagents, DNA Constructs and Antibodies

Preparation and use of ECM ligands have been previously described (18). DNA plasmids for expression of GFP alone or Trop-2-GFP in PC3-MM2 cells were previously described (15). DNA plasmid for expression of a Trop-2 variant devoid of the cytoplasmic tail (Δcyto Trop-2) was a kind gift of Dr. S. Alberti. siRNA to Trop-2 were from Dharmacon (SMARTPool: L-010609-00). Tetramethyl rhodamine isothiocyanate (TRITC)-conjugated phalloidin (Sigma-Aldrich) was used for staining of actin cytoskeleton. All primary and secondary Abs used in this study are listed in Supplementary Table S1.

Cells and Culture Conditions

Cell lines, culture conditions and generation of cell transfectants have been previously described (18). Authentication of the cell lines was provided with their purchase from American Type Culture Collection; cells were used in our laboratory for less than 6 months. PC3-MM2 cells (tested, authenticated by fingerprinting and provided by Dr. Sue-Hwa Lin, The University of Texas M.D. Anderson Cancer Center) were cultured in DMEM supplemented with 10% FBS, 1% non-essential aminoacids, 1 mmol/L sodium pyruvate.

Generation of Protein Lysates

Cell lysates were prepared by scraping cells in 20 mM Tris-HCl (pH 7.4), 150 mmol/L NaCl, 1 mmol/L $CaCl_2$, 1 mmol/L $MgCl_2$ 1% Brij-97, 1 mmol/L benzamidine, 10 μg/mL leupeptin, 1 mmol/L phenylmethylsulfonyl fluoride, 1 μg/mL pepstatin A, 1 μmol/L calpain inhibitor, 1 mmol/L Na_3VO_4, 1 mmol/L $Na_4O_7P_2$. After 15 minutes incubation on ice, lysates were centrifuged at 12,000 g for 10 minutes. Supernatants were collected and protein content was determined using the DC Protein Assay Kit (Bio-Rad). Samples were subjected to 10% SDS-PAGE under reducing conditions and transferred onto polyvinylidene difluoride membranes for immunoblotting (IB).

Immunoprecipitation (IP)

IP experiments were performed as follows: cells were lysed in the lysis buffer described above and pre-clearing was performed by two consecutive incubations with protein G-Sepharose at 4°C for 45 minutes. Binding to specific Abs was performed by incubation at 4°C for 3 hours, followed by incubation with protein G-Sepharose at 4°C for 1 hour. After six washes with lysis buffer, immunocomplexes were eluted with 100 mmol/L glycine pH 2.5, followed by pH neutralization using Tris to a final concentration of 50 mmol/L. The immunocomplexes were then separated by SDS-PAGE. For integrin activation experiments, IP was performed lysing PC3-1 cells after extensive washes with PBS without Ca^{2+}/Mg^{2+}, followed by incubation with PBS supplemented with 0.2 mM $MnCl_2$ at 37°C for 10 minutes. Ligand-dependent association was assayed seeding PC3-1 cells on FN, VN or collagen-I, followed by lysis and processing as described above. Cells were lysed after exposure to the

various ligands for different amounts of time (FN, 40 minutes; vitronectin (VN), 75 minutes; collagen-I, 15 minutes) in order to ensure comparable rate of spreading, as determined by light microscopy analysis.

Rho GTPase Activation Assays

Rac1 and Rho activation experiments were performed using the specific, non-radioactive kits from Millipore (#17–441 and #17–294), following the manufacturer's instructions. PC3-1/ctr. shRNA, PC3-1/Trop-2 shRNA, PC3-2/Mock and PC3-2/Trop-2 cells were seeded on FN for 60 min before lysis and processing for detection of Rac1-GTP and Rho-GTP.

Cell Migration Assay

Transwell chambers (12 μm pore diameter, Costar) were coated with FN (10 μg/mL) or VN (10 μg/mL) overnight at 4°C. After cell detachment and trypsin inactivation, cells were seeded on coated transwell chambers at 37°C for 5 hours. After fixation with 3.7% paraformaldehyde (PFA), cells attached on both layers of the porous filter were stained with 1 μg/mL 4',6-diamidino-2-phenylindole (DAPI) and pictures of nuclei were acquired by fluorescence microscopy (Olympus IX71 or Nikon Eclipse TS-100 inverted microscopes equipped with fluorescence unit). Then, cells on the top layer were removed using a cotton swab, and pictures of nuclei from cells migrated to the bottom layer were acquired. Five and twenty random fields were acquired for quantification of attached and migrated cells, respectively. Cell Profiler software (www.cellprofiler.org) was used for quantification of nuclei number, using 10–30 pixel units as range for discrimination between single nuclei and potential aggregates. The ratio between number of cells migrated onto the bottom layer and total (top + bottom) number of cells attached on the filter was calculated for each group of transfectants. AIIB2, an inhibitory Ab to β_1, was used at the concentration of 30 μg/10^6 cells to perform migration assays on PC3-2 transfectants. A non-immune rat IgG was used as a negative control Ab at the same concentration as AIIB2. The assays were repeated at least three times, and similar results were observed. Chi-Square test was used for statistical analysis.

Live Cell Microscopy Analysis of Cell Movements on FN

PC3-2 and LNCaP cell transfectants were seeded at 2×10^4 cells/mL and allowed to spread for 3 hours on FN in 24-well plates. Cell movements were monitored using a widefield live cell imaging system: images were acquired on a Zeiss live cell imaging system (Axiovert 200M, Carl Zeiss) using a 20× objective and a Coolsnap HQ CCD monochrome camera (Roper) at 10-minute intervals for 17 hours. A programmable X,Y,Z stage (Prior Proscan III) was used for acquisition of multiple positions and stitching of large areas. Cells were maintained at 37°C in a humidified 5% (v/v) CO_2 atmosphere during the time course using a dedicated environmental chamber (Okolab). Images were then converted to stacks using ImageJ, and migration tracks of non-dividing, non-clustered cells were manually obtained using the Manual Tracking (http://rsb.info.nih.gov/ij/plugins/track/track.html) and the Chemotaxis and Migration Tool (version 1.01; Ibidi GmbH, Martinsried, Germany; http://ibidi.com/software/chemotaxis_and_migration_tool/?x21b49=6f65b0702c4bf44855c8e20d1b340358) ImageJ plugins. Directionality (persistence) was determined by dividing the linear displacement of a cell after 17 hours by the total distance moved, where migration in a straight line equals to a directionality of 1. Migration paths in four randomly chosen fields were tracked in duplicate wells for each cell type. The significance of changes in directionality, velocity, total distance and linear displacement was determined using a Student's T test.

Animal model of cancer cell dissemination

All experiments were conducted in accordance with NIH guidelines for the humane use of animals. All protocols involving the use of animals were approved by the Drexel University College of Medicine Committee for the Use and Care of Animals. Six-to-eight week-old male SCID mice were anesthetized with 100 mg/kg ketamine and 20 mg/kg xylazine and successively inoculated in the left cardiac ventricle with PC3-MM2 cell transfectants (2.5×10^5 cells in a volume of 100 μL of serum-free DMEM). Cell inoculation was performed with an insulin syringe with a 30-gauge needle. Blue-fluorescent polystyrene beads (10 μm diameter, Invitrogen-Molecular Probes) were co-injected with cancer cells, and their detection by fluorescence microscopy in different organs at necropsy confirmed the successful inoculation in the systemic blood circulation. Mice were sacrificed at 2 weeks following inoculation and tissues prepared as described below.

Livers were collected and fixed in 4% PFA for 24 hours and then transferred into fresh PFA for additional 24 hours. Tissues were frozen in Optimal Cutting Temperature (OCT) medium (Electron Microscopy Sciences) by placement over dry ice-chilled 2-methylbutane (Fisher). 80 μm thick sections were obtained using a Microm HM550 cryostat (Mikron Instruments). Twenty seven sections were cut from each liver, and analyzed by fluorescence microscopy.

Bright-field and fluorescent images of cancer cells homing to the liver parenchyma were acquired using an upright microscope (AX10, Carl Zeiss) coupled to a Multispectral Imaging System (CRI). Spectral deconvolution was applied to fluorescence images using the Nuance Software (v. 2.4), in order to generate color-coded digital images. Two investigators (M.T. and L.R.L.) analyzed and counted the number of metastatic foci.

Immunofluorescence (IF) and Confocal Microscopy

Cells were seeded on FN-coated glass coverslips for 1 hour at 37°C. Then, fixation with 3.7% PFA was performed for 15 minutes at room temperature, followed by quencing with 50 mmol/L NH_4Cl. Cells were permeabilized by incubation with PBS / 0.2% Triton X-100 for 5 minutes, and then incubated for 30 minutes at room temperature with the blocking solution (PBS / 5% BSA). Single staining and/or co-staining were performed incubating samples with primary Abs for 20 minutes at room temperature, followed by incubation with secondary Abs (Alexa Fluor 488-Rabbit anti mouse and/or Alexa Fluor 633-Donkey anti goat) for 20 minutes at room temperature. After three washes, coverslips were mounted on glass slides using Pro-Long anti-fade reagent (Invitrogen), and slides were analyzed on an inverted confocal microscope (LSM510, Carl Zeiss) using Plan-Apochromat 63× (1.4 NA) or Plan-Neofluar 100× (1.3 NA) lenses. Staining for visualization of talin in focal adhesions and membrane rims was performed on adhesive structures (cell ghosts), obtained by osmotic shock of cells seeded on FN. Briefly, the FN-adherent cells were rinsed with PBS, then incubated in H_2O for 1 minute to osmotically disrupt the cells, and quickly flushed to shear away the dorsal membranes. The structures were then fixed in 3.7% PFA and processed for staining and IF analysis.

Immunohistochemical Analysis

Metastatic specimens consisted of prostate tumors from the following locations: liver, lung, retro-peritoneal soft tissue, portal Lymph Nodes (LNs), para-aortic LNs, mesenteric LNs, pulmonary hilar LNs, pelvic LNs, dura, spleen, adrenal glands, kidney, pleura, pancreas and bladder. The tissues were formalin-fixed and paraffin-embedded, then a Tissue Microarray (TMAs) was constructed with three cores (0.6 mm in diameter) taken from each representative block, as described in (20). Tissue samples were collected after “rapid” autopsies at the University of Michigan Hospitals under Institutional Review Board

approved protocols. Autopsies have been referred to as “rapid” or “warm” because of the short time interval between patient death and necropsy. Staining by immunohistochemistry (IHC) was conducted using a goat polyclonal Ab (pAb) to Trop-2, as described in (16).

Results

Trop-2 expression induces metastatic dissemination of prostate cancer cells in animal models and is abundant in human prostate cancer metastasis

We have shown that Trop-2 inhibits prostate cancer cell adhesion to FN in vitro by modulation of the β_1 integrin-RACK1-FAK-Src signaling axis (18). Here, we investigated the effect of Trop-2 expression in vivo. We utilized PC3-MM2 cells, previously characterized to depend on β_1 integrins for metastatic growth in various organs (S.H. Lin, personal communication). Since these cells do not express Trop-2 endogenously, we generated stable transfectants expressing green fluorescent protein (GFP) alone or Trop-2-GFP (Supplementary Fig. S1A). We injected these transfectants in the arterial circulation of Severe Combined Immunodeficiency (SCID) mice via left cardiac ventricle and analyzed liver sections (n=27/mouse) after 2 weeks in order to detect fluorescent foci. Using spectral deconvolution on fluorescence microscopy sections we obtained color-coded pictures (Supplementary Fig. S1B), that were analyzed for detection of cells penetrated in the liver parenchyma (Fig. 1A). We detect a total of 53 foci in the Trop-2-GFP group (n=4 mice), as compared with 9 foci detected in the control group (n=4 mice). Since overexpression of Trop-2 promotes prostate cancer metastatic dissemination in preclinical models (Fig. 1A), we investigated the relevance of these findings in human prostate cancer metastasis. We analyzed Trop-2 expression levels in human prostate cancer metastasis by IHC. We used TMAs containing 120 cores obtained from 40 “rapid” autopsy specimens (20). Analysis of three cores representative of each of the 40 “rapid” autopsy specimens (120 cores total), shows that, as depicted in Fig. 1B, expression of Trop-2 is found in all distant metastases analyzed, including liver, LNs, lung, pancreas, retro-peritoneal soft tissue, and dura metastasis. This evidence demonstrates an active role for Trop-2 in prostate cancer metastatic dissemination.

Trop-2 stimulates β_1 integrin-dependent directional migration of prostate cancer cells

We investigated the effect of Trop-2 on integrin-mediated cell migration using PC3-2/Trop-2 transfectants and DU145/Trop-2 small hairpin RNA (shRNA) cells (18) seeded on FN- and VN-coated transwell plates (Fig. 2A and 2B). The percentage of PC3-2/Trop-2 cells migrated on FN (48.4±4.2%) is significantly higher than Mock (13.0±4.9%) and β_5 (12.3±4.9%) transfectants (Fig. 2A and Supplementary Fig. S2A). On the other hand, the percentage of PC3-2/Trop-2 cells migrated on VN (26.5±5.1%) is similar to that of Mock (21.4±4.9%) or β_5 (20.9±5.4%) transfectants (Fig. 2A). Consistent with a role for Trop-2 as a promoter of integrin-mediated migration, we observe strong reduction of DU145 migration on FN (Fig. 2B) upon shRNA-mediated silencing of Trop-2 (18). The percentage of DU145/Trop-2 shRNA cells migrated on FN (22.3±4.6%) is indeed significantly smaller than parental cells (54.8±5.1%). In contrast, the percentage of DU145/Trop-2 shRNA cells migrated on VN (31.0±2.2%) does not change as compared with parental cells (25.8±3.0%). Altogether, these data demonstrate that the anti-adhesive function of Trop-2 (18) results in an enhanced migratory phenotype of prostate cancer cells, and this effect is selectively detectable when cells are seeded on FN. The contribution of Trop-2 to prostate cancer cell migration is completely reverted in the presence of AIIB2, an inhibitory Ab to β_1, indicating that β_1 integrins are the mediators of Trop-2-dependent cell-ECM interactions (Fig. 2C). We also analyzed velocity, distance and directionality of PC3-2 (Fig. 2D) and LNCaP (Supplementary Fig. S2B) transfectants seeded on FN-coated plates by observing their migration paths over 17 hours. The velocity of PC3-2/Trop-2 cells (4.6±0.2 μm/hour) is

significantly higher than that of Mock (2.9±0.1 μm/hour) transfectants. The directionality of PC3-2/Trop-2 (0.63±0.02) migration is also significantly increased as compared with that of Mock (0.46±0.02) cells (Fig. 2D). Similar evidence was obtained using LNCaP cell transfectants. The velocity of LNCaP/Trop-2 cells (9.6±0.3 μm/hour) is significantly higher than that of Mock (6.9±0.3 μm/hour) transfectants. The directionality of LNCaP/Trop-2 (0.47±0.02) migration is also significantly increased as compared with that of Mock (0.29±0.02) cells (Supplementary Fig. S2B). We observe lower levels of Rac1-GTP in PC3-2/Trop-2 as compared with Mock transfectants, as well as higher levels of Rac1-GTP in PC3-1/Trop-2 shRNA as compared with control shRNA (ctr. shRNA) cells seeded on FN (Fig. 2E). These findings are in agreement with previous reports showing that enhanced directional migration results from suppression of Rac1 activity in the peripheral lamellae and specific accumulation of active Rac1 in the axial leading edges (21). Thus, Trop-2 appears to stimulate directional migration by modulating important signaling pathways at the leading edges.

Trop-2 co-localizes with β_1 integrins at the leading edges of prostate cancer cells

We have previously shown that Trop-2 does not affect expression or ion-mediated activation of β_1 (18). β_1 integrins are part of the focal adhesion platforms and contribute to stabilize cell attachment to ECM ligands (22). Therefore, we hypothesized that Trop-2 affects β_1 functions by interfering with recruitment of these receptors into focal adhesions. We achieved stable silencing of Trop-2 in endogenously expressing PC3-1 cells using shRNA (Fig. 3A), and stable ectopic expression of this molecule by transfecting PC3-2 cells with the human *TROP2* cDNA [Fig. 3B and (18)]. Then, we seeded PC3-1/Trop-2 shRNA cells and PC3-2/Trop-2 transfectants on FN and performed immunofluorescence (IF) analysis to detect the subcellular distribution of various integrin receptors. In PC3-1, we observe localization of β_1 in focal adhesions of Trop-2 shRNA cells, whereas these receptors are accumulated in the membrane of ctr. shRNA cells (Fig. 3C, left). In these cells, the average number of β_1-containing focal adhesions is 78.2±4.5/cell in Trop-2 shRNA cells (focal adhesions, n=2,504/32 cells) as compared with 7.5±1.1/cell in ctr. shRNA cells (focal adhesions, n=240/32 cells) (Fig. 3C, right). The localization of α_v integrins in focal adhesions is unaffected upon silencing of Trop-2 (Fig. 3C, left); the number of α_v-containing focal adhesions is indeed 55±2.9/cell in Trop-2 shRNA cells (focal adhesions, n=993/18 cells) as compared with 47±4.9/cell in ctr. shRNA cells (focal adhesions, n=985/21 cells) (Fig. 3C, right). In PC3-2 cell transfectants we observe localization of β_1 in the membrane of Trop-2-expressing cells and predominant distribution of these receptors in peripheral and ventral focal adhesions of Mock cells (Fig. 3D, left). The average number of β_1-containing focal adhesions is 27.2±6.2/cell in Trop-2 transfectants (focal adhesions, n=545/20 cells) as compared with 79.4±9.2/cell in Mock cells (focal adhesions, n=1,350/17 cells) (Fig. 3D, right). In these cells, the localization of β_3 integrin in focal adhesions is unchanged upon ectopic expression of Trop-2 (Fig. 3D, left). Indeed, the number of β_3-containing focal adhesions is 35±6/cell (focal adhesions, n=841/24 cells) in PC3-2/Trop-2 as compared with 48±10/cell (focal adhesions, n=530/11 cells) in PC3-2/Mock cells (Fig. 3D, right). These effects are unlikely to depend on a non-physiological amount of Trop-2 obtained upon transfection, as its expression levels in PC3-2 (Fig. 3B) transfectants are similar to the endogenous levels detected in PC3-1 (18). We further verified that these effects are not due to changes in other integrin subunit expression; similar to β_1 (Supplementary Fig. S3A and S3B, left panels), surface levels of β_3 (Supplementary Fig. S3A, right) and α_v (Supplementary Fig. S3B, right) integrin subunits are unaffected by Trop-2.

Strong co-localization between Trop-2 and β_1 in discrete membrane compartments is observed in both parental PC3-1 cells (endogenously expressing Trop-2) and PC3-2

transfectants (Fig. 4A). As expected, we do not detect any co-localization of Trop-2 with β_5 (Fig. 4A), which is uniformly distributed on the cell surface in agreement with previous reports (23). As shown in Fig. 4B, we observe strong co-localization of Trop-2 with the phosphorylated form of Akt (pAkt) which is frequently accumulated at the leading edges of actively migrating cells (24). Using PC3-2/Trop-2 (Fig. 4C, left) and DU145/Trop-2 cells transfected with small interfering RNA (siRNA) (Fig. 4C, right), we also find that Trop-2 stimulates the phosphorylation of p21-activated kinase 4 (PAK4), a kinase that is localized at the leading edges of migratory cells and promotes focal adhesion turnover by inhibiting the formation of mature, large focal adhesions in DU145 cells migrating on FN (25). Overall, our findings suggest that the anti-adhesive function of Trop-2 leads to enhanced migration of prostate cancer cells on ECM ligands through accumulation of β_1 integrins in the leading edges and reduced localization in focal adhesions. In support of our evidence obtained by IF microscopy (Fig. 4A), co-immunoprecipitation (co-IP) assays performed using parental PC3-1 cells and LNCaP transfectants also reveal interaction between β_1 and Trop-2 (Fig. 4D). This association is specific, as we do not detect any interaction between Trop-2 and β_3 (Fig. 4E). We performed IP of β_1 integrins upon stimulation of PC3-1 cells with Mn^{2+} ions (Supplementary Fig. S4A), which are known to induce a conformational switch in the β_1 extracellular domain, leading to activation of the molecule by exposure of the cation-and-ligand-influenced binding site (CLIBS) epitopes (18). Furthermore, we immunoprecipitated β_1 integrins upon seeding of PC3-1 cells on FN, VN or collagen-I (Supplementary Fig. S4B) in order to detect ligand-dependent effects. Comparable amount of the Trop-2/β_1 complex is detected in all experimental conditions tested, suggesting the existence of a binding interface exposed and available for the interaction of Trop-2 and β_1 integrins at all time.

Overall, these data suggest that a novel Trop-2/β_1 complex is responsible for preferential accumulation of β_1 in the leading edges of cells seeded on FN, and consequently enhanced cell migration on this ECM ligand.

The $\alpha_5\beta_1$ integrin heterodimer is accumulated in the leading edges in response to Trop-2 expression

Among the integrin heterodimers able to bind FN, $\alpha_5\beta_1$ integrin plays a critical role in inducing invasive phenotypes (10). Therefore, we assessed whether the localization of the α_5 subunit reflected the Trop-2-dependent distribution of β_1 in focal adhesions or leading edges of prostate cancer cells seeded on FN. As shown in Fig. 5A (left), we observe that α_5 integrin is indeed relocalized in leading edges of PC3-2 cells upon ectopic expression of Trop-2. The average number of α_5-containing focal adhesions is 5.0±0.7/cell in Trop-2 transfectants (focal adhesions, n=92/20 cells) as compared with 51.0±1.9/cell in Mock cells (focal adhesions, n=1,544/30 cells) (Fig. 5A, right). Similar to the other integrin subunits, surface levels of α_5 are unchanged upon expression of Trop-2 (Supplementary Fig. S3C). Co-localization of Trop-2 with α_5 is observed at the leading edges of both Trop-2 endogenously (DU145) and exogenously (PC3-2) expressing cells seeded on FN (Fig. 5B). On the other hand, α_v integrins, extensively accumulated in focal adhesions, do not co-localize with Trop-2, which is never found in these structures (Fig. 5C). This observation is further confirmed by IP of the α_v subunit, followed by IB analysis of Trop-2 and β_1 (Fig. 5D). Integrins are continuously internalized from and recycled to the plasma membrane, and Rab4- and Rab11-positive compartments are major routes of this trafficking cycle (26). Upon induction of membrane receptor trafficking, we observe localization of Trop-2 in Rab4- and Rab11-positive vesicles (Supplementary Fig. S5A). We also find co-localization between Trop-2 and $\alpha_5\beta_1$ integrin in both internalization (Supplementary Fig. S5B, top) and recycling (Supplementary Fig. S5B, bottom) vesicles. This suggests that Trop-2 forms a

complex with $\alpha_5\beta_1$ during trafficking from/to plasma membrane and facilitates localization of $\alpha_5\beta_1$ at the leading edges preventing accumulation in focal adhesions.

Trop-2 binds the β_1 / talin complex, which is relocalized to the cell membrane

Functionally, a Trop-2-mediated redistribution of β_1 may impact on cytoskeletal dynamics and focal adhesion turnover. The focal adhesion proteins vinculin and talin mediate a link between integrins and the actin cytoskeleton, and contribute to the modulation of cytoskeletal dynamics. Recent evidence highlighted the importance of talin during prostate cancer progression, since this protein induces migration in vitro and metastasis in vivo (27). Binding of talin to the integrin cytoplasmic tail is mediated by the N-terminal head domain (talin-H) (28), which is generated upon cleavage of the full length (FL) talin by intracellular calcium-dependent proteases, calpains and has been reported to promote focal adhesion turnover and cell migration (29). As shown in Fig. 6A, we observe an interaction between Trop-2 and talin-H by co-IP using PC3-2/Mock and PC3-2/Trop-2 transfectants. Moreover, talin is no longer accumulated in focal adhesions in PC3-2 cells upon ectopic expression of Trop-2, as observed by IF staining of adhesive structures (n=50 cells/group), designated as cellular ghosts (Fig. 6B). On the other hand, vinculin, which directly binds F-actin and is more tightly associated with focal adhesions than talin, remains localized in these platforms independently on the presence of Trop-2 (Fig. 6C). Furthermore, we observe increased association between β_1 and talin-H in presence of Trop-2 as compared with negative control cells (Fig. 6D). An additional set of experiments was performed to characterize the interaction of Trop-2 with β_1 and talin. A Trop-2 variant devoid of the cytoplasmic tail (Δcyto Trop-2) was transfected in PC3-2 cells (Supplementary Fig. S6) and IP of Trop-2 was performed in order to detect β_1 and talin. We observe that the amount of β_1 integrins and talin-H co-immunoprecipitated with wild type Trop-2 is similar to that detected in the immunoprecipitates of Δcyto Trop-2 (Fig. 6E). This suggests that the cytoplasmic tail of Trop-2 is not involved in the association with talin, and that the binding to β_1 integrins occurs through their extracellular domains. Furthermore, in support of an indirect, β_1-dependent binding, the association between Trop-2 and talin is compromised upon silencing of β_1 (data not shown). We do not detect binding of Trop-2 to either FL-talin (Fig. 6E) or the adaptor molecule Kindlin-1 (Fig. 6F), suggesting that the association may occur in other stages of adhesion dynamics, when the calpain-mediated cleavage of talin determines accelerated focal adhesion turnover and induces destabilization of cell attachment to the ECM ligand (29, 30). We prove that the actin cytoskeleton dynamics is indeed affected in prostate cancer cells by Trop-2; as shown in Fig. 7, staining of PC3-1/ctr. shRNA and PC3-1/Trop-2 shRNA cells with phalloidin-TRITC reveals a strikingly different distribution of the stress fibers. In particular, the actin cytoskeleton is accumulated at the leading edge of PC3-1/ctr. shRNA seeded on FN, and colocalizes with both Trop-2 and β_1 integrins throughout the entire cell thickness, as depicted by the representative ventral and dorsal cell layers (Fig. 7, top panels). On the other hand, long radial stress fibers appear in the ventral side of PC3-1/Trop-2 shRNA cells (Fig. 7, bottom panels); these findings are in agreement with recent reports, showing that radial stress fibers are responsible for stabilizing focal adhesions over long times and slowing their disassembly (31).

In summary, our data indicate that the $\alpha_5\beta_1$/talin complex is rapidly destabilized from its localization inside the focal adhesion platform in highly motile, Trop-2-expressing cells. A molecular association of Trop-2 with the $\alpha_5\beta_1$/talin complex redirects these proteins to the leading edges, counteracting the full maturation of focal adhesions. The resulting weak focal adhesions (where vinculin remains localized) cause detachment of cancer cells from the tumor ECM, enhancing migration and metastatic dissemination.

Discussion

In this study, we demonstrate for the first time that Trop-2, an anti-adhesive transmembrane protein that is frequently upregulated in human carcinomas, promotes metastatic dissemination of prostate cancer cells in vivo. These findings are relevant to human cancer since we observe abundant expression of Trop-2 in human prostate cancer metastasis, indicating that this molecule may be a key driver of prostate cancer progression. We also show here that Trop-2 promotes cancer cell migration on FN, a phenomenon dependent on β_1 integrins, through relocalization of the $\alpha_5\beta_1$ heterodimer and of its associated protein talin from focal adhesions to the leading edges.

Our data support the notion that inhibiting cancer cell adhesion to FN facilitates detachment from the tumor mass, where FN is known to be largely expressed (32, 33), and dissemination toward distant organs; moreover, our findings reveal a novel role for Trop-2 as a driver of this event. This proposed role for Trop-2 during the early phases of cancer progression complements indeed a recent study by Zijlstra et al., who reported that stabilization of focal adhesions induced by a specific Ab targeting the tetraspanin CD151 results in increased cell immobility as well as reduced migration in vitro and departure of cancer cells from the primary site in vivo (34). However, Wang et al. have provided unexpected evidence that loss of Trop-2 promotes epithelial-to-mesenchymal transition in a model of skin cancer obtained by exposure of *Arf*-null mice to the carcinogen DMBA-TPA, that induces oncogenic mutations in the *H-Ras* gene (35). As suggested by the authors, downregulation of Trop-2 appears to be restricted to the sarcomatoid subset of human head and neck squamous cell carcinomas which has lost epithelial characteristics (35). Our results, instead, appear consistent with most studies, showing positive correlation between Trop-2 overexpression and poor prognosis in several human carcinomas (15).

Mechanistically, we prove here that Trop-2 associates with and induces relocalization of β_1, but not β_3 integrins at the leading edges, counteracting their accumulation in mature focal adhesions and consequently promoting migration of prostate cancer cells on FN. Persistence of β_1 integrins in focal adhesions has been reported to enhance resistance to motility (22), whereas localization at the leading edges promotes cell migration (36, 37). This evidence, and the fact that β_1 integrins are differentially localized in normal prostate versus prostate cancer tissues (9), suggests a significant pathologic relevance of our findings. β_1 integrins can be dynamically redistributed in subcellular compartments (38), and these events are modulated by several mechanisms, including tyrosine phosphorylation (39). Moreover, integrin functions are regulated by cross-talks with other transmembrane receptors. Among other examples, CD47/IAP interacts with several integrin isoforms (40) and modulates cell migration on their ligands through G_i proteins; a cross-talk between epidermal growth factor receptor and β_1 integrins has also been reported to promote the transformed phenotype of breast cancer cells in 3D microenvironments (41). Thus, our study provides evidence that transmembrane proteins without enzymatic (e.g. kinase) activity, such as Trop-2, regulate β_1 integrin redistribution at the leading edges of carcinoma cells seeded on FN.

We demonstrate that Trop-2 stimulates the activity of PAK4, a kinase that enhances focal adhesion turnover in prostate cancer cells seeded on FN (25) and mediates cancer cell dissemination via a cross-talk with Src (42). Since Trop-2 controls the β_1 integrin-RACK1-FAK-Src signaling axis (18), a critical regulator of focal adhesion turnover and cell adhesion (43), our data indicate a potential role for PAK4 as downstream effector of the β_1 integrin/Trop-2 complex. PAK kinases are known to mediate cell migration on ECM acting as effectors of Rho GTPases (Rho, Rac, Cdc42) (44), which regulate β_1-dependent actin/actomyosin dynamics (45). We show that Trop-2 promotes directional cell migration, a process largely dependent on a balanced activity of Rac1 at the axial leading edge (21).

Our findings also show that Trop-2 induces reorganization of the actin cytoskeleton and selective removal of talin from focal adhesions. The association of talin with phosphatidylinositol 4,5-biphosphate [PI(4,5)P_2] is a prerequisite for talin/integrin binding, since PI(4,5)P_2 exposes integrin-binding sites on talin (46). Recently, the PI(4,5)P_2-synthesizing enzyme, PIPKIγ, has been shown to critically modulate polarized integrin accumulation at the leading edge and directional cell migration (47). PIPKIγ forms a complex with talin, and this interaction enhances the binding of β_1 integrins to talin at the leading edge, given the accumulation of PI(4,5)P_2 in this compartment. PIPKIγ is recruited to the plasma membrane by electrostatic interactions between a positively charged flat surface of the molecule and the negatively charged phosphatidic acid in the plasma membrane (48). Although the molecular mechanisms underlying our findings that Trop-2 enhances the association between β_1 and talin (Fig. 6) remain to be fully elucidated, they may involve co-translocation of Trop-2 and PIPKIγ to membrane ruffles at the leading edge. Indeed, the C-ter portion of the Trop-2 cytoplasmic tail comprises an α-helix rich in Glu residues, that may interact with the cytosolic pool of PIPKIγ during translocation to the leading edge. We also demonstrate that both wild type and Δcyto Trop-2 co-immunoprecipitate with β_1 and talin-H, suggesting that the extracellular region of Trop-2 mediates binding to the β_1/talin complex (Fig. 6). We did not observe co-IP between Trop-2 and FL-talin, indicating that the interaction with β_1/talin may take place upon generation of talin-H, due to the intracellular, calcium-dependent proteases, calpains. These enzymes play a crucial role in promoting cell migration, as they counteract excessive stabilization of focal adhesions (29). Since Trop-2 is a calcium signal transducer (49), a contribution of this molecule in destabilization of focal adhesion through accelerated activation of calpains may be hypothesized. However, future studies are needed to address these various possibilities.

Although Trop-2 expression does not alter either protein levels or activity of β_1 integrins in prostate cancer cells (18), we observe that these two proteins associate in a novel complex and co-localize in trafficking vesicles; since we never detect Trop-2 in focal adhesions, co-recycling to leading edges from intra-cytoplasmic compartments is likely to represent a potential mechanism underlying the Trop-2-dependent phenotype observed in this study. Among other integrin subunits we analyzed Trop-2 effect on α_5 integrin, which associates with β_1 to form the major FN receptor. We find that Trop-2 also co-localizes with α_5 integrin at the leading edges and induces redistribution of this integrin subunit from focal adhesions to these membrane compartments, without affecting its surface levels. Migratory and invasive phenotypes of cancer cells may be modulated by changing $\alpha_5\beta_1$ expression levels or function (10, 11); our findings show that cancer cell motility may be also enhanced by relocalizing this integrin heterodimer from focal adhesions to membrane ruffles at the leading edge. A potential mechanism to explain this Trop-2-dependent phenotype may involve integrin trafficking pathways, since recycling vesicles have been reported to increase the invasive properties of tumor cells (50).

In summary, we describe here a novel mechanism underlying prostate cancer cell migration on ECM components through a molecular cross-talk between Trop-2, $\alpha_5\beta_1$ integrin and talin.

Supplementary Material

Refer to Web version on PubMed Central for supplementary material.

Acknowledgments

We thank S. Alberti, L. Borgia, E. Cuckierman, T. de Angelis, A. Dutta, C. Fedele, R. Galanti, K. Ganguly, H.L. Goel, E. Guerra, A. Sayeed and T. Wang for constructive discussion; S. Alberti, E. Ruoslahti and C. Has for

antibodies; S. Alberti for the DNA plasmid encoding for Δcyto Trop-2; SH. Lin for the PC3-MM2 cells. We also thank Y. Covarrubias and J.H. Keen for constructive suggestions and technical support in bioimaging experiments.

Grant Support

This work was supported by the following grants: NIH-R01CA109874, NIH-R01CA089720 and NIH-P01CA140043 to L.R.L.; NIH-SPORE in Prostate Cancer 2 P50 CA69568 to J.S. (PI: KJ. Pienta); Italian Association for Cancer Research (AIRC) Fellowship to M.T.

Research in this publication includes work carried out using the Kimmel Cancer Center Bioimaging Facility and the Translational Research & Pathology Shared Resource, which are supported in part by NCI Cancer Center Support Grant P30 CA56036. This project is also funded, in part, under a Commonwealth University Research Enhancement Program grant with the Pennsylvania Department of Health (H.R.). The Department specifically disclaims responsibility for any analyses, interpretations or conclusions.

Abbreviations

ECM	extracellular matrix
FN	fibronectin
VN	vitronectin
IP	immunoprecipitation
IB	immunoblotting
IF	immunofluorescence
FACS	flow cytometry
IHC	immunohistochemistry
PI(4,5)P_2	phosphatidylinositol 4,5-biphosphate
PAK4	p21-activated kinase 4
shRNA	small hairpin RNA
siRNA	small interfering RNA
pAkt	phospho-Akt
FL-talin	full length talin
talin-H	talin head
TRITC	tetramethyl rhodamine isothiocyanate
FITC	fluorescein isothiocyanate
Ab	antibody
mAb	monoclonal Ab
pAb	polyclonal Ab
PFA	paraformaldehyde
PCC	Pearson's correlation coefficient
GFP	green fluorescent protein
FAK	focal adhesion kinase

References

1. Siegel R, Naishadham D, Jemal A. Cancer statistics. CA Cancer J Clin. 2013; 63:11–30. [PubMed: 23335087]

2. Lu P, Weaver VM, Werb Z. The extracellular matrix: a dynamic niche in cancer progression. J Cell Biol. 2012; 196:395–406. [PubMed: 22351925]
3. Zhu H, Zhao J, Zhu B, Collazo J, Gal J, Shi P, et al. EMMPRIN regulates cytoskeleton reorganization and cell adhesion in prostate cancer. Prostate. 2012; 72:72–81. [PubMed: 21563192]
4. Lokeshwar VB, Cerwinka WH, Isoyama T, Lokeshwar BL. HYAL1 hyaluronidase in prostate cancer: a tumor promoter and suppressor. Cancer Res. 2005; 65:7782–7789. [PubMed: 16140946]
5. Hynes RO. Integrins: bidirectional, allosteric signaling machines. Cell. 2002; 110:673–687. [PubMed: 12297042]
6. Kanchanawong P, Shtengel G, Pasapera AM, Ramko EB, Davidson MW, Hess HF, et al. Nanoscale architecture of integrin-based cell adhesions. Nature. 2010; 468:580–584. [PubMed: 21107430]
7. Demetriou MC, Cress AE. Integrin clipping: a novel adhesion switch? J Cell Biochem. 2004; 91:26–35. [PubMed: 14689578]
8. Fornaro M, Manes T, Languino LR. Integrins and prostate cancer metastases. Cancer Metastasis Rev. 2001; 20:321–331. [PubMed: 12085969]
9. Knox JD, Cress AE, Clark V, Manriquez L, Affinito KS, Dalkin BL, et al. Differential expression of extracellular matrix molecules and the α6-integrins in the normal and neoplastic prostate. Am J Pathol. 1994; 145:167–174. [PubMed: 8030747]
10. Mierke CT, Frey B, Fellner M, Herrmann M, Fabry B. Integrin α5β1 facilitates cancer cell invasion through enhanced contractile forces. J Cell Sci. 2011; 124:369–383. [PubMed: 21224397]
11. Chen J, De S, Brainard J, Byzova TV. Metastatic properties of prostate cancer cells are controlled by VEGF. Cell Commun Adhes. 2004; 11:1–11. [PubMed: 15500293]
12. Chong JM, Speicher DW. Determination of disulfide bond assignments and N-glycosylation sites of the human gastrointestinal carcinoma antigen GA733-2 (CO17-1A, EGP, KS1-4, KSA, and Ep-CAM). J Biol Chem. 2001; 276:5804–5813. [PubMed: 11080501]
13. Ciccarelli FD, Acciarito A, Alberti S. Large and diverse numbers of human diseases with HIKE mutations. Hum Mol Genet. 2000; 9:1001–1007. [PubMed: 10767324]
14. Nakatsukasa M, Kawasaki S, Yamasaki K, Fukuoka H, Matsuda A, Tsujikawa M, et al. Tumor-associated calcium signal transducer 2 is required for the proper subcellular localization of claudin 1 and 7: implications in the pathogenesis of gelatinous drop-like corneal dystrophy. Am J Pathol. 2010; 177:1344–1355. [PubMed: 20651236]
15. Trerotola M, Cantanelli P, Guerra E, Tripaldi R, Aloisi AL, Bonasera V, et al. Up-regulation of Trop-2 quantitatively stimulates human cancer growth. Oncogene. 2012 [published online ahead of print February 20, 2012].
16. Trerotola M, Rathore S, Goel HL, Li J, Alberti S, Piantelli M, et al. CD133, Trop-2 and α2β1 integrin surface receptors as markers of putative human prostate cancer stem cells. Am J Transl Res. 2010; 2:135–144. [PubMed: 20407603]
17. Goldstein AS, Lawson DA, Cheng D, Sun W, Garraway IP, Witte ON. Trop2 identifies a subpopulation of murine and human prostate basal cells with stem cell characteristics. Proc Natl Acad Sci USA. 2008; 105:20882–20887. [PubMed: 19088204]
18. Trerotola M, Li J, Alberti S, Languino LR. Trop-2 inhibits prostate cancer cell adhesion to fibronectin through the β1 integrin-RACK1 axis. J Cell Physiol. 2012; 227:3670–3677. [PubMed: 22378065]
19. Takaoka M, Nakamura T, Ban Y, Kinoshita S. Phenotypic investigation of cell junction-related proteins in gelatinous drop-like corneal dystrophy. Invest Ophthalmol Vis Sci. 2007; 48:1095–1101. [PubMed: 17325151]
20. Rubin MA, Putzi M, Mucci N, Smith DC, Wojno K, Korenchuk S, et al. Rapid ("warm") autopsy study for procurement of metastatic prostate cancer. Clin Cancer Res. 2000; 6:1038–1045. [PubMed: 10741732]
21. Pankov R, Endo Y, Even-Ram S, Araki M, Clark K, Cukierman E, et al. A Rac switch regulates random versus directionally persistent cell migration. J Cell Biol. 2005; 170:793–802. [PubMed: 16129786]
22. Roca-Cusachs P, Gauthier NC, Del Rio A, Sheetz MP. Clustering of α5β1 integrins determines adhesion strength whereas αvβ3 and talin enable mechanotransduction. Proc Natl Acad Sci USA. 2009; 106:16245–16250. [PubMed: 19805288]

23. Wayner EA, Orlando RA, Cheresh DA. Integrins αvβ3 and αvβ5 contribute to cell attachment to vitronectin but differentially distribute on the cell surface. J Cell Biol. 1991; 113:919–929. [PubMed: 1709170]
24. Higuchi M, Onishi K, Kikuchi C, Gotoh Y. Scaffolding function of PAK in the PDK1-Akt pathway. Nat Cell Biol. 2008; 10:1356–1364. [PubMed: 18931661]
25. Wells CM, Whale AD, Parsons M, Masters JR, Jones GE. PAK4: a pluripotent kinase that regulates prostate cancer cell adhesion. J Cell Sci. 2010; 123:1663–1673. [PubMed: 20406887]
26. Xia B, Joubert A, Groves B, Vo K, Ashraf D, Djavaherian D, et al. Modulation of cell adhesion and migration by the histone methyltransferase subunit mDpy-30 and its interacting proteins. PLoS One. 2010; 5:e11771. [PubMed: 20668708]
27. Sakamoto S, McCann RO, Dhir R, Kyprianou N. Talin1 Promotes Tumor Invasion and Metastasis via Focal Adhesion Signaling and Anoikis Resistance. Cancer Res. 2010; 70:1885–1895. [PubMed: 20160039]
28. Anthis NJ, Wegener KL, Critchley DR, Campbell ID. Structural diversity in integrin/talin interactions. Structure. 2010; 18:1654–1666. [PubMed: 21134644]
29. Franco SJ, Rodgers MA, Perrin BJ, Han J, Bennin DA, Critchley DR, et al. Calpain-mediated proteolysis of talin regulates adhesion dynamics. Nat Cell Biol. 2004; 6:977–983. [PubMed: 15448700]
30. Huang C, Rajfur Z, Yousefi N, Chen Z, Jacobson K, Ginsberg MH. Talin phosphorylation by Cdk5 regulates Smurf1-mediated talin head ubiquitylation and cell migration. Nat Cell Biol. 2009; 11:624–630. [PubMed: 19363486]
31. Oakes PW, Beckham Y, Stricker J, Gardel ML. Tension is required but not sufficient for focal adhesion maturation without a stress fiber template. J Cell Biol. 2012; 196:363–374. [PubMed: 22291038]
32. Soikkeli J, Podlasz P, Yin M, Nummela P, Jahkola T, Virolainen S, et al. Metastatic outgrowth encompasses COL-I, FN1, and POSTN up-regulation and assembly to fibrillar networks regulating cell adhesion, migration, and growth. Am J Pathol. 2010; 177:387–403. [PubMed: 20489157]
33. Naba A, Clauser KR, Hoersch S, Liu H, Carr SA, Hynes RO. The matrisome: in silico definition and in vivo characterization by proteomics of normal and tumor extracellular matrices. Mol Cell Proteomics. 2012; 11:M111. 014647. [PubMed: 22159717]
34. Zijlstra A, Lewis J, Degryse B, Stuhlmann H, Quigley JP. The inhibition of tumor cell intravasation and subsequent metastasis via regulation of in vivo tumor cell motility by the tetraspanin CD151. Cancer Cell. 2008; 13:221–234. [PubMed: 18328426]
35. Wang J, Zhang K, Grabowska D, Li A, Dong Y, Day R, et al. Loss of Trop2 Promotes Carcinogenesis and Features of Epithelial to Mesenchymal Transition in Squamous Cell Carcinoma. Mol Cancer Res. 2011; 9:1686–1695. [PubMed: 21970857]
36. Puklin-Faucher E, Sheetz MP. The mechanical integrin cycle. J Cell Sci. 2009; 122:179–186. [PubMed: 19118210]
37. Tuomi S, Mai A, Nevo J, Laine JO, Vilkki V, Ohman TJ, et al. PKCε regulation of an α5 integrin-ZO-1 complex controls lamellae formation in migrating cancer cells. Sci Signal. 2009; 2:ra32. [PubMed: 19567915]
38. Singer II, Scott S, Kawka DW, Kazazis DM, Gailit J, Ruoslahti E. Cell surface distribution of fibronectin and vitronectin receptors depends on substrate composition and extracellular matrix accumulation. J Cell Biol. 1988; 106:2171–2182. [PubMed: 2454933]
39. Johansson MW, Larsson E, Luning B, Pasquale EB, Ruoslahti E. Altered localization and cytoplasmic domain-binding properties of tyrosine-phosphorylated β1 integrin. J Cell Biol. 1994; 126:1299–1309. [PubMed: 7520449]
40. Brown EJ, Frazier WA. Integrin-associated protein (CD47) and its ligands. Trends Cell Biol. 2001; 11:130–135. [PubMed: 11306274]
41. Wang F, Weaver VM, Petersen OW, Larabell CA, Dedhar S, Briand P, et al. Reciprocal interactions between β1-integrin and epidermal growth factor receptor in three-dimensional basement membrane breast cultures: a different perspective in epithelial biology. Proc Natl Acad Sci USA. 1998; 95:14821–14826. [PubMed: 9843973]

42. Siu MK, Chan HY, Kong DS, Wong ES, Wong OG, Ngan HY, et al. p21-activated kinase 4 regulates ovarian cancer cell proliferation, migration, and invasion and contributes to poor prognosis in patients. Proc Natl Acad Sci USA. 2010; 107:18622–18627. [PubMed: 20926745]
43. Cox BD, Natarajan M, Stettner MR, Gladson CL. New concepts regarding focal adhesion kinase promotion of cell migration and proliferation. J Cell Biochem. 2006; 99:35–52. [PubMed: 16823799]
44. Kumar R, Gururaj AE, Barnes CJ. p21-activated kinases in cancer. Nat Rev Cancer. 2006; 6:459–471. [PubMed: 16723992]
45. Hirsch E, Barberis L, Brancaccio M, Azzolino O, Xu D, Kyriakis JM, et al. Defective Rac-mediated proliferation and survival after targeted mutation of the β1 integrin cytodomain. J Cell Biol. 2002; 157:481–492. [PubMed: 11980921]
46. Martel V, Racaud-Sultan C, Dupe S, Marie C, Paulhe F, Galmiche A, et al. Conformation, localization, and integrin binding of talin depend on its interaction with phosphoinositides. J Biol Chem. 2001; 276:21217–21227. [PubMed: 11279249]
47. Thapa N, Sun Y, Schramp M, Choi S, Ling K, Anderson RA. Phosphoinositide signaling regulates the exocyst complex and polarized integrin trafficking in directionally migrating cells. Dev Cell. 2012; 22:116–130. [PubMed: 22264730]
48. Roach AN, Wang Z, Wu P, Zhang F, Chan RB, Yonekubo Y, et al. Phosphatidic acid regulation of PIPKI is critical for actin cytoskeletal reorganization. J Lipid Res. 2012; 53:2598–2609. [PubMed: 22991193]
49. Ripani E, Sacchetti A, Corda D, Alberti S. Human Trop-2 is a tumor-associated calcium signal transducer. Int J Cancer. 1998; 76:671–676. [PubMed: 9610724]
50. Caswell PT, Spence HJ, Parsons M, White DP, Clark K, Cheng KW, et al. Rab25 associates with α5β1 integrin to promote invasive migration in 3D microenvironments. Dev Cell. 2007; 13:496–510. [PubMed: 17925226]

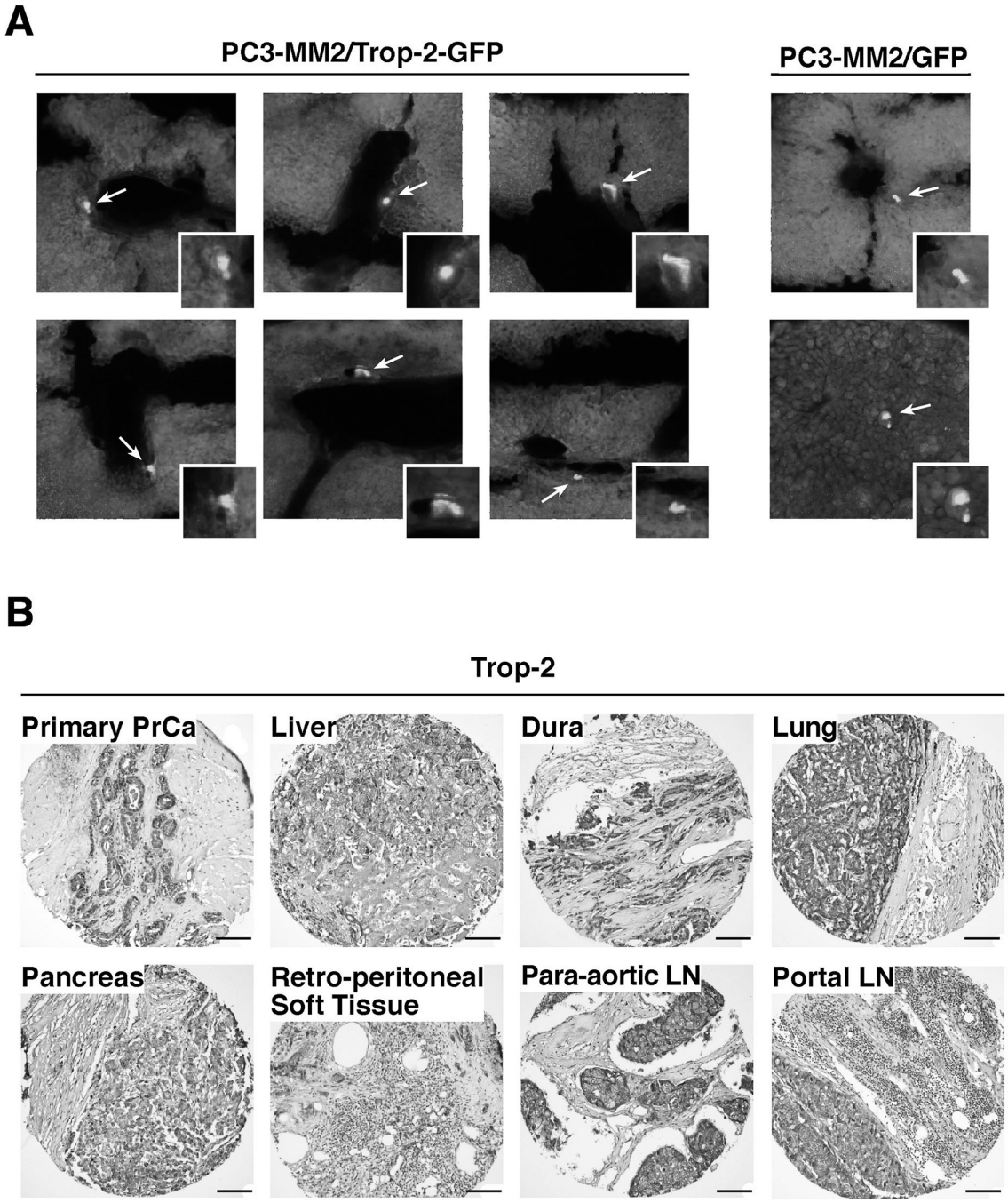

Figure 1.

Trop-2 induces prostate cancer cell dissemination in vivo and is abundantly expressed in human prostate cancer metastasis. A, PC3-MM2/Trop-2-GFP and PC3-MM2/GFP were injected in the left cardiac ventricle of SCID mice, and the presence of fluorescent cells in livers was quantified after 2 weeks. Representative pictures of PC3-MM2/Trop-2-GFP (left) and PC3-MM2/GFP (right) cells in the liver parenchyma are shown. Arrows and magnification boxes, fluorescent cells. B, Representative IHC images of Trop-2 expression in liver, dura, lung, pancreas, retro-peritoneal soft tissue, para-aortic LN and portal LN metastasis from prostate cancer patients are shown. Bars, 100 μm.

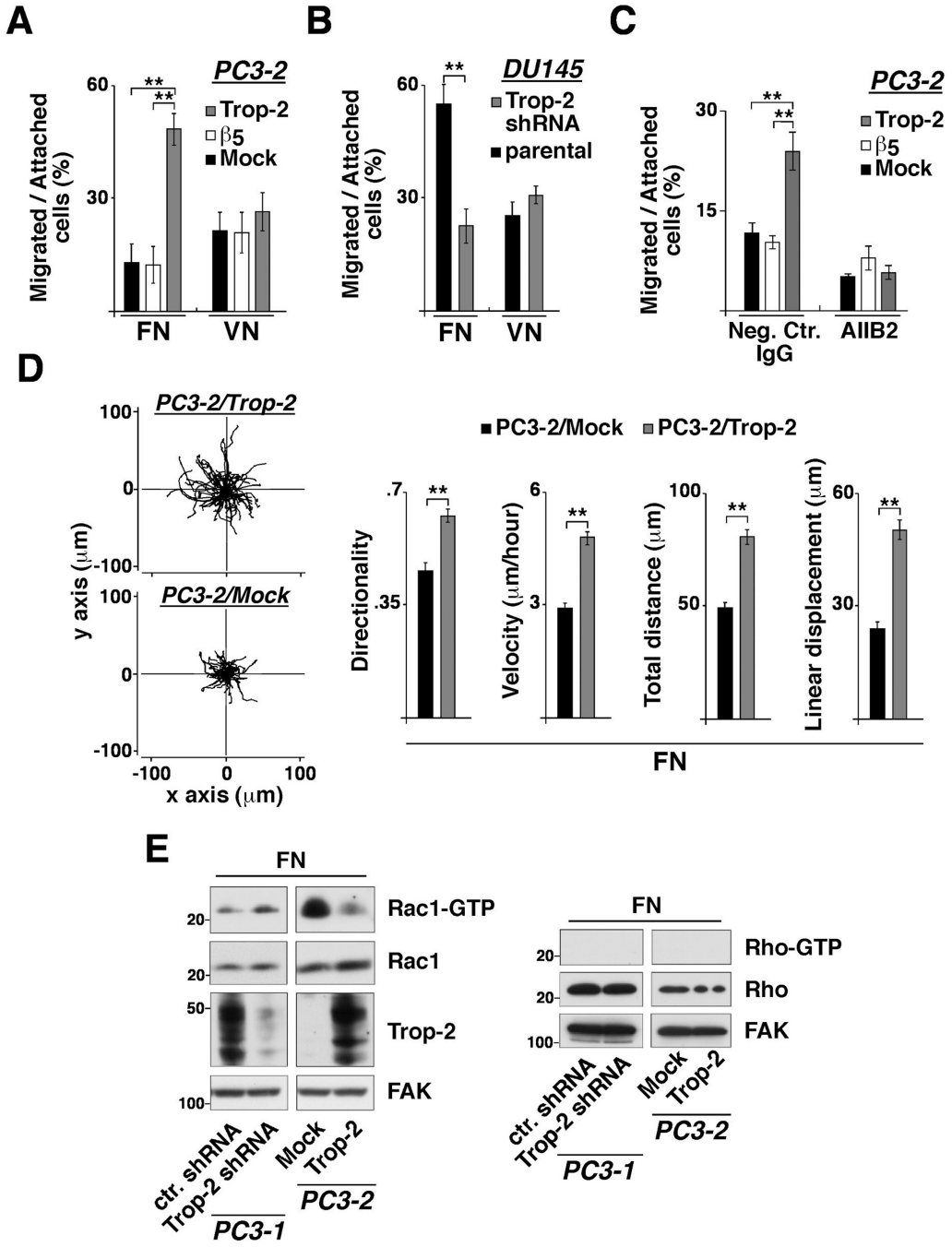

Figure 2.

β_1 integrin-dependent prostate cancer cell migration is enhanced by Trop-2. A, Migration assays were performed using PC3-2 transfectants seeded on FN- or VN-coated transwell chambers, as described in Materials and Methods. The fraction of cells migrated onto the bottom layer was calculated for each group of transfectants and expressed as percentage of total number of cells attached on both filter layers. Error bars, SEM. **, P<0.001. B, Migration assays were also performed using DU145/Trop-2 shRNA versus parental DU145 cells seeded on FN- or VN-coated transwell chambers. Error bars, SEM. **, P<0.001. C, Migration of PC3-2 transfectants on FN was assessed in the presence of AIIB2, an inhibitory Ab to β_1 integrins. A non-immune rat IgG was used as negative control Ab. **, P<0.001. D,

PC3-2/Trop-2 (top) and PC3-2/Mock (bottom) transfectants seeded on FN-coated plates were observed for 17 hours by time-lapse video microscopy; the movements of individual cells were followed using cell-tracking software, and the panels are presented as overlays of trajectories described by cells during their migration (left). Bar graphs show directionality, velocity, total distance migrated and linear displacement of PC3-2/Trop-2 (n=63 cells) and PC3-2/Mock (n=68 cells) transfectants extracted from the trajectories (right). Values are reported as means ± SEM. **, $P<0.001$. E, Rac1-GTP (left) and Rho-GTP (right) levels were measured in PC3-1/Trop-2 shRNA and ctr. shRNA cells, as well as in PC3-2/Trop-2 and Mock transfectants seeded on FN. Trop-2 expression was quantified in both groups of cell lines tested for Rac1 and Rho activity. FAK, control of protein loading.

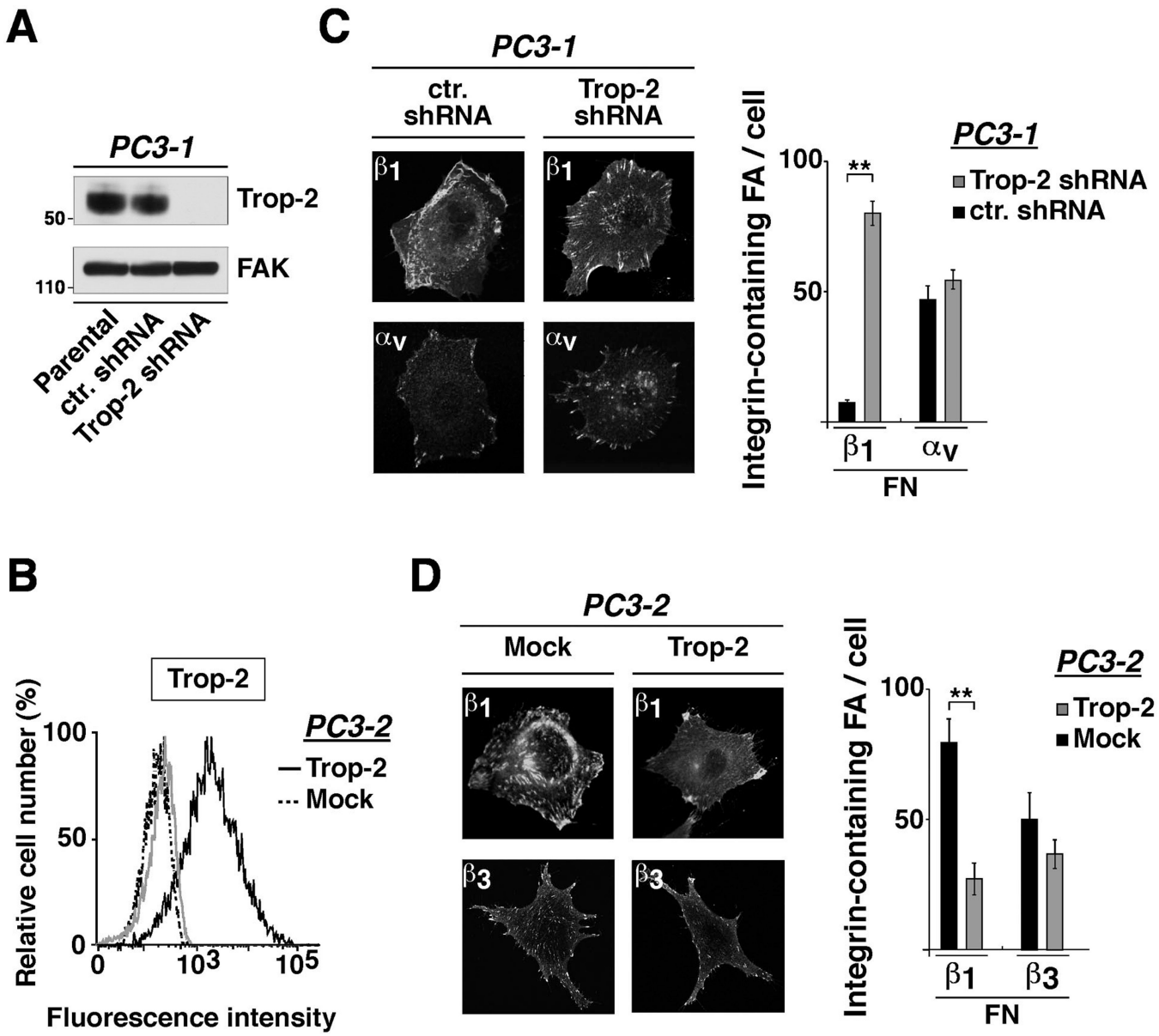

Figure 3.

β_1 integrins are localized at the leading edges rather than focal adhesions in Trop-2 expressing cells. A, Trop-2 expression was evaluated by IB after shRNA-mediated silencing in PC3-1 cells. FAK, control of protein loading. B, Trop-2 expression levels in PC3-2 transfectants were evaluated by FACS (continuous black line). PC3-2/Mock stained with an Ab to Trop-2 (dotted black line), and PC3-2/Trop-2 stained with a non-immune mouse IgG (continuous gray line) were used as negative controls. C, Localization of β_1 and α_v in PC3-1/ctr. shRNA and PC3-1/Trop-2 shRNA cells seeded on FN was analyzed by IF (left). β_1- and α_v-containing focal adhesions were counted, and average numbers/cell are shown in the bar graph (right). Error bars, SEM. **, P<0.001. D, Localization of β_1 and β_3 integrins in PC3-2/Mock and PC3-2/Trop-2 transfectants seeded on FN was analyzed by IF (left). β_1- and β_3-containing focal adhesions were counted in the two groups of transfectants, and average numbers/cell are shown in the bar graph (right). Error bars, SEM. **, P<0.001.

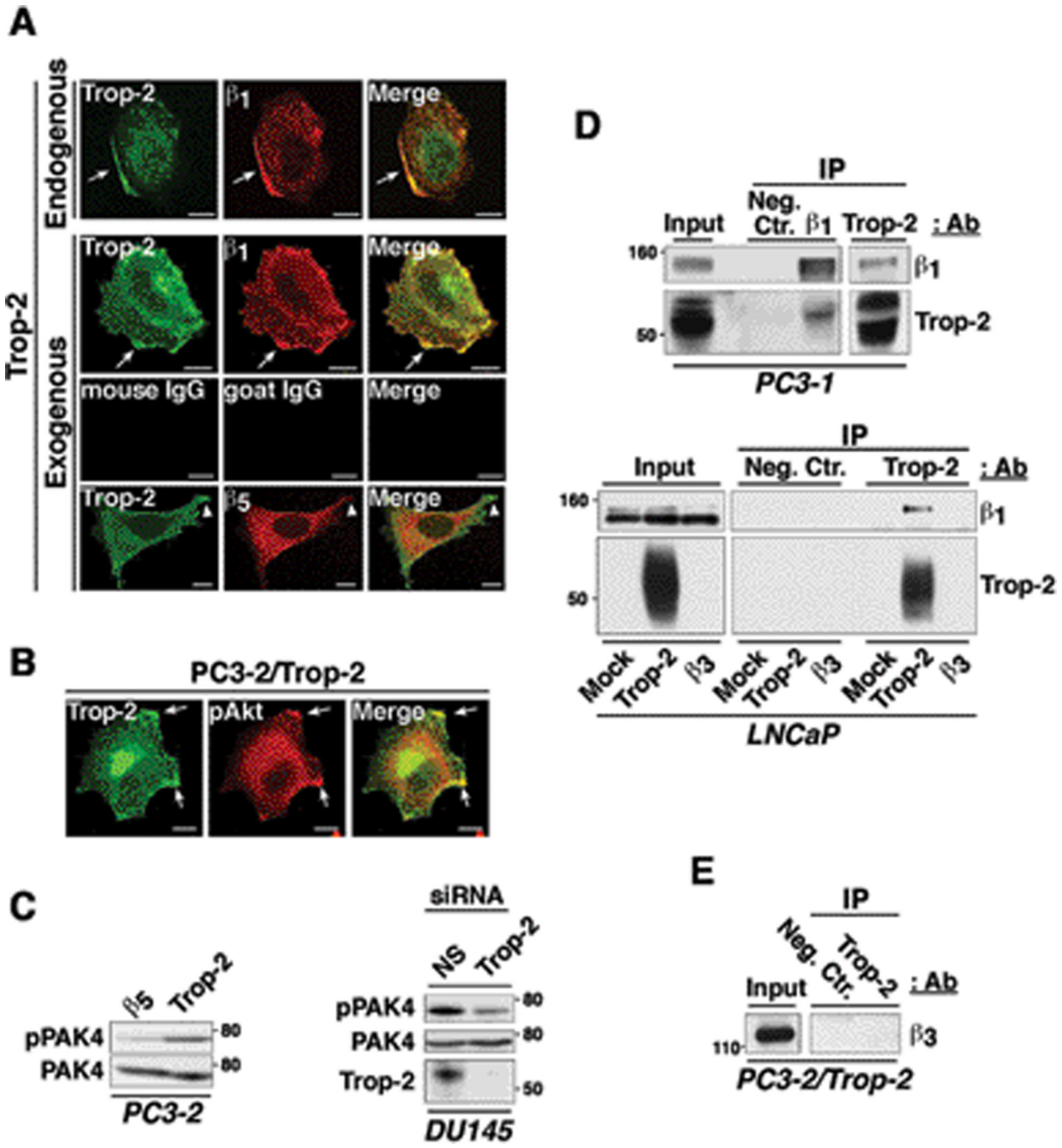

Figure 4.

The Trop-2/β_1 integrin complex is accumulated in the leading edges of prostate cancer cells seeded on FN. A, PC3-1 cells, endogenously expressing Trop-2 (first row from top), and PC3-2/Trop-2 transfectants (second row from top) were seeded on FN and stained for Trop-2 (green) and β_1 integrins (red). Arrows show co-localization of β_1 and Trop-2 in membrane rims at the leading edges. Mouse IgG and goat IgG, negative control Abs for Trop-2 and β_1, respectively (third row from top). PC3-2/Trop-2 transfectants seeded on FN were also stained for Trop-2 and β_5 integrin. Arrowheads show Trop-2-containing membrane protrusions (green), with undetectable co-localization of β_5 (red) (bottom row). B, PC3-2/Trop-2-GFP (green) transfectants were seeded on FN, then fixed and stained with

an Ab to pAkt (Ser473) (red). Arrows, leading edges. A and B, Bars, 10 μm. C, Phosphorylation of PAK4 was analyzed by comparing PC3-2/Trop-2 transfectants with negative control cells (PC3-2/β_5) (left). Phosphorylation of PAK4 was also analyzed in DU145 cells upon siRNA-mediated silencing of Trop-2. A non-silencing (NS) siRNA was used as negative control (right). Total PAK4, control of protein loading. D, β_1 integrins and Trop-2 were immunoprecipitated from PC3-1 protein lysates; the immunoprecipitates were then analyzed by IB using a goat pAb against Trop-2 and a mAb against β_1 integrins, respectively (top). Trop-2 was immunoprecipitated from LNCaP transfectant lysates, and the immunoprecipitates were then analyzed by IB using a goat pAb against β_1 integrins. LNCaP/Trop-2 transfectants were compared with Mock or β_3 integrin transfectants (bottom). E, Trop-2 was immunoprecipitated from PC3-2/Trop-2 cell lysates, and IB analysis was performed on the immunoprecipitates using an Ab against β_3 integrin. D and E, A mouse IgG (Neg.Ctr.) was used as a negative control Ab for IP.

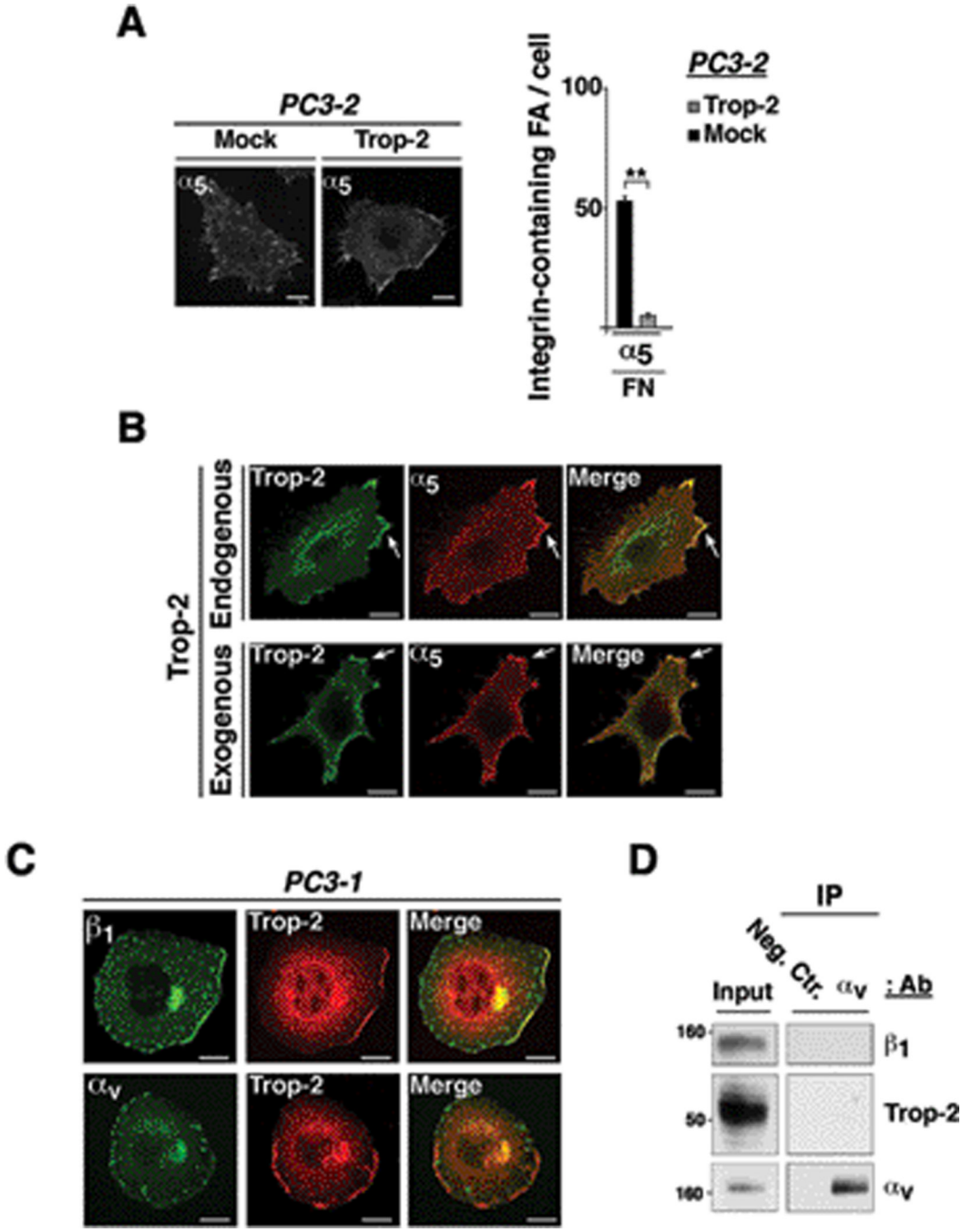

Figure 5.

$\alpha_5\beta_1$ integrin is accumulated in the leading edges of Trop-2 expressing cells. A, Localization of α_5 in PC3-2/Mock and PC3-2/Trop-2 cells seeded on FN was analyzed by IF (left). α_5-containing focal adhesions were counted, and average numbers/cell are shown in the bar graph (right). Error bars, SEM. **, P<0.001. B, DU145 cells, endogenously expressing Trop-2 (top panels), and PC3-2/Trop-2 transfectants (bottom panels) were seeded on FN and stained for Trop-2 (green) and α_5 (red). Arrows show co-localization of α_5 and Trop-2 in membrane rims at the leading edges. C, PC3-1 cells were seeded on FN, and co-localization of Trop-2 with β_1 or α_v integrins at the leading edges was assessed by confocal microscopy. A, B and C, Bars, 10 μm. D, PC3-1 cell lysates were immunoprecipitated using

an Ab targeting α_v integrins; β_1, Trop-2 and α_v were then detected by IB. A non-immune mouse IgG was used as a negative control Ab (Neg. Ctr.).

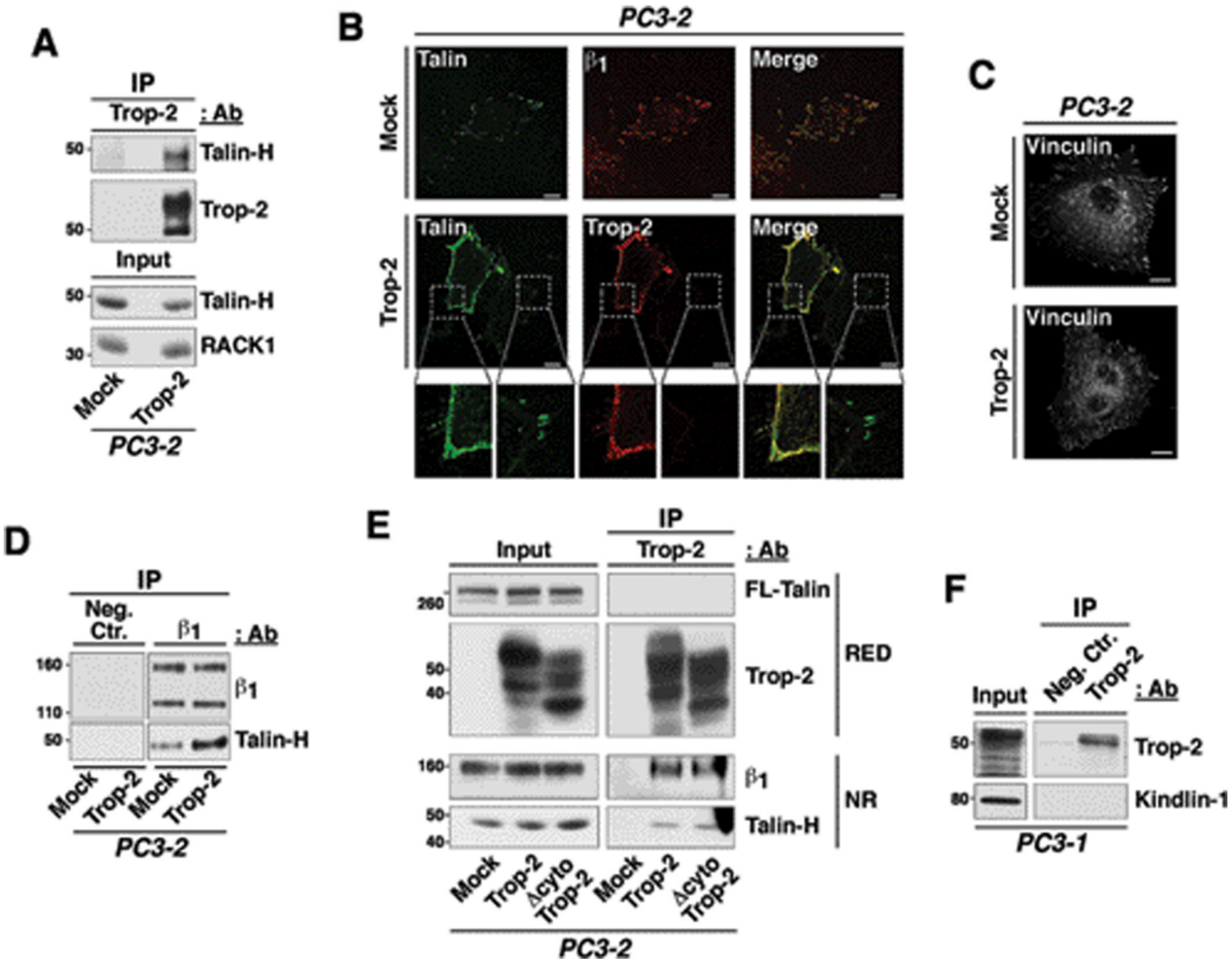

Figure 6.

Trop-2 co-precipitates with and induces relocalization of talin from focal adhesions to cell edges. A, Trop-2 was immunoprecipitated from PC3-2/Mock and PC3-2/Trop-2 lysates; the immunoprecipitates were separated by non reducing SDS-PAGE and analyzed by IB using an anti talin-H Ab. B, Localization of talin was analyzed in ghosts of Mock and Trop-2 transfectants of PC3-2 cells, seeded on FN. Talin (green) is localized in focal adhesions of Mock cells, where β_1 integrins (red) are also found (top panels). In Trop-2 transfectants, talin is localized in membrane rims together with Trop-2 (red) (middle panels). Magnified boxes show details of talin (green) localization in membrane rims and focal adhesions (bottom). Trop-2 localization in membrane rims is also shown (red). C, PC3-2/Mock and PC3-2/Trop-2 transfectants were seeded on FN, and then stained for vinculin. Localization of vinculin in peripheral and ventral focal adhesions is shown. B and C, Bars, 10 μm. D, β_1 integrins were immunoprecipitated from PC3-2/Mock and PC3-2/Trop-2 protein lysates; the immunoprecipitates were then analyzed by IB in order to detect talin-H. A mouse IgG (Neg.Ctr.) was used as a negative control Ab for IP. E, Trop-2 was immunoprecipitated from PC3-2/Mock, PC3-2/Trop-2 and PC3-2/Δcyto Trop-2 protein lysates, and IB analysis was performed on the immunoprecipitates using mAbs against FL-talin and talin-H, and goat pAbs against Trop-2 and β_1 integrins. RED, SDS-PAGE performed in reducing conditions. NR, SDS-PAGE performed in non-reducing conditions. F, Trop-2 was

immunoprecipitated from PC3-1 protein lysates, and IB analysis was performed on the immunoprecipitates using a rabbit pAb against Kindlin-1. A mouse IgG (Neg.Ctr.) was used as a negative control Ab for IP.

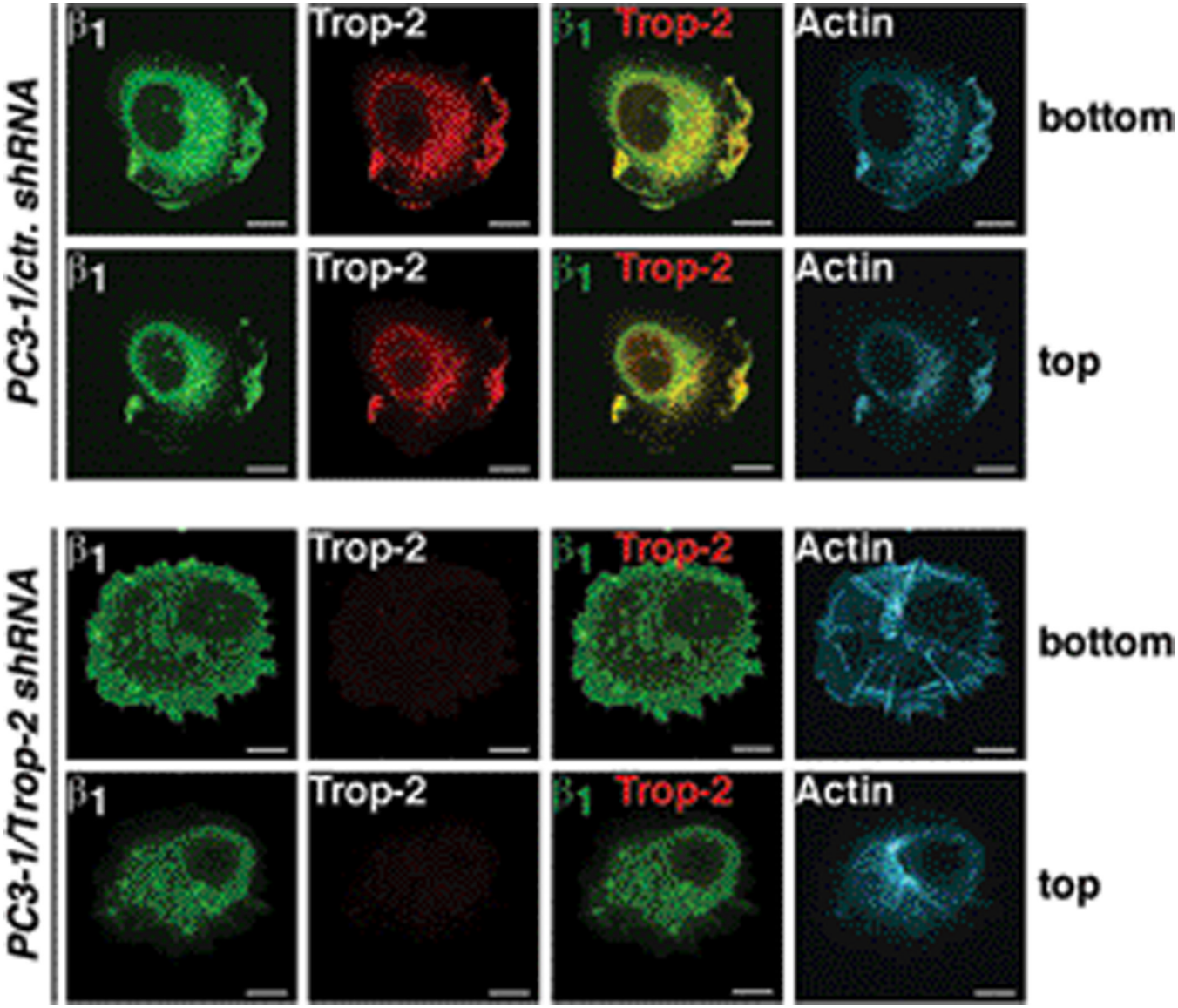

Figure 7.

Trop-2-dependent reorganization of actin cytoskeleton. PC3-1/ctr. shRNA (top rows) and PC3-1/Trop-2 shRNA (bottom rows) cells were stained with Abs against β_1 integrins (green) and Trop-2 (red), as well as with phalloidin-TRITC in order to observe the actin cytoskeleton (cyan). Ventral (bottom) and dorsal (top) cell layers are shown.